Physico-chemical Characterization, Structuration and Morphology of Photo-active Heterojunction (P3HT-PCBM) used in Organic Photovoltaic Cells

S. Hamham, S. Belaaouad and Y. Naimi
Laboratory chemical chemistry of materials Hassan II University Faculty of Science Ben M'sik Department of Chemistry, Morocco

Keywords: Photoactive Layer, Lamellar Structuration, Quasi-crystalline Fibrils, Nanocrystals PCBM, Electron Donor Acceptor Interface.

Abstract: In this paper, we propose a study on the physicochemical, morphological and structural characterization of the organic semiconductors (P3HT) (poly-3-hexylthiophene) and the (PC61BM) ([6,6] - phenyl - C61 - butyric acid methyl ester), as well as their structuration in lamellae of quasi-crystalline fibrils for the first one and in Nano-crystals for the second. These conformational transitions that the two macromolecules undergo allow their self-assembly in chlorobenzene into a photoactive donor-electron acceptor layer. By controlling the morphology of the layer, its film deposition on the electrodes and its orientation with respect to which, a donor charge transfers optimization (P3HT) is favoured to the PC61BM acceptor which aims to improve the efficiency of the organic photovoltaic cells.

1 INTRODUCTION

The study and characterization of the physicochemical properties of semiconducting materials based on conjugated polymers has been the subject of numerous studies, however, we are faced with a panoply of problems and difficulties posed by their use which are far to be solved and continue to receive increased attention and research (Destruel and Seguy, 2007), (Vanlaeke *et al.*, 2006), (Baran *et al.*, 2017).

The materials of choice on which we will focus this study, will be P3HT (poly (3-hexylthiophene)) as electron donor and PC61BM ([6.6] -phenyl-C61-butyric acid methyl ester) as electron acceptor (Berson *et al.*, 2007). Which will be used to develop a one-dimensional network of organization, structure and shape thus optimizing the charge transfer by opting for the low oxidation potential of the donor, which results in the reduction of the width of the forbidden band. In addition, the presence of the σ_π_σ bonds, which lead to the conjugation of the chain, and constitute traps for the electrons, which are essential to preserve the structuration and organization of the P3HT-PC61BM, network which is necessary for the transport of Frenkelexcitons of small radius because of the low dielectric constant of the two materials (Björström*et al.*, 2005), (Brabec *et al.*, 2010), (Alet *et al.*, 2006).

Therefore, the purification and obtaining of high molecular weight polymers and high regio-regularity is the key to the development of the ordered structure network and the electron-donor-acceptor interface. Different techniques for preparing, characterizing and depositing the active layer on the substrate and on the electrodes in order to obtain the volume heterojunction capable of collecting the photons and generating the excitons, which will dissociate into charge carriers. These processes will provide access to pure polymers, their molecular weight, their chemical, electrochemical, thermal, electrical and optical properties, and finally to their optimum size and shape ensuring their self-assembly in order volume heterojunction providing access to improved energy conversion efficiency of organic photovoltaic cells (Chen *et al.*, 2011), (Dang, Hirsch and Wantz, 2011), (Rispens*et al.*, 2003), (Peumans, Yakimov and Forrest, 2003).

Hamham, S., Belaaouad, S. and Naimi, Y.
Physico-chemical Characterization, Structuration and Morphology of Photo-active Heterojunction (P3ht-Pcbm) Used In Organic Photovoltaic Cells.
DOI: 10.5220/0009776102180225
In *Proceedings of the 1st International Conference of Computer Science and Renewable Energies (ICCSRE 2018)*, pages 218-225
ISBN: 978-989-758-431-2

2 SYNTHESIS AND CHARACTERIZATION OF THE ACTIVE LAYER

2.1 P3HT Donor Material

2.1.1 Synthesis and Spectroscopic Characterization

The synthesis is carried out starting from a starting material, which is 3bromo- 4-methylthiophene-C11 in two stages starting from 4 g of the reagent, an alkylation followed by an aromatic nucleophilic substitution in the presence of Cu (I), then the brominated derivatives are purified by evaporation after isolation by chlorobenzene extraction of 3 hexyloxytiophene. For the polymerization, several processes are possible: Electrochemical polymerization, polymerization by chemical coupling of two aromatic rings catalyzed by complexes with transition metals, or opt for the polymerization by oxidizing chemical means the presence of (FeCl3, MoCl5, RuCl3) and then eliminates the mineral impurities methanol hot followed by training via a cyclohexane washing and finally proceeded to a purification by washing with soxhlet.

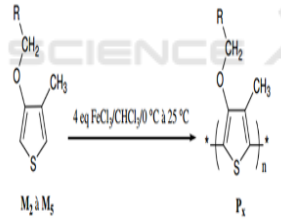

Polymer P_x	R	Efficiency %
P_2	$-(CH_2)_7-CH_3$	26
P_3	$-(CH_2)_4-CH_3$	59
P_4	$-(CF_2)_7-CF_3$	52
P_5	$-(CF_2)_4-CF_3$	61

Figure 1: Synthesis scheme and polymerization yields of P2 to P5.

After extraction of the polymers with dichloromethane or with chloroform, the compound is isolated by filtration-centrifugation. And in order to control the regioregularity due to the presence of hexyl and hexyloxyl chains which conditions the electrical and photovoltaic properties of the P3HT by, playing either on the temperature of the reaction or the steric hindrance, and it is found that the longer the polymer chain is, the higher its molecular weight, and the greater the degree of regioregularity which allows the polymeric chains of organize in ordered lamellar structure of fibrils, which are detected by UV absorption spectroscopy, and the resistance of fibril amalgams (lamellae) which is due to the interaction between the lateral alkyl chains is confirmed by 1 H NMR spectroscopy, the aromatic protons close to the thiophene ring junctions are influenced by these and the aliphatic protons of CH3 and CH2 are influenced by the couplings, which makes it possible to observe the existence of long chains, thus of high molecular weight, and this gives them a high degree of regioregularity.

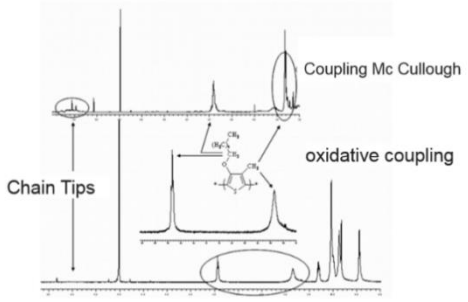

Figure 2: Comparison of the proton NMR spectra in tetrachloroethane of poly (3-hexyloxy-4-methylthiophene) obtained by chemical coupling of Mc Cullough P3't type by oxidative coupling P3.

2.1.2 Measurement of the Molar Mass of P3HT

Many techniques are existing for determination of molar mass of macromolecules in solution for example: viscosimetry, osmometry, polyacrylamid gel electrophoresis PAGE, static light scattering SLS, steric exclusion chromatography SEC, relaxation time visco-elastometry RTVE and ultracentrifugation ...etc.

The molar mass is obtained specially by measurements of the viscoelastic relaxation time expressed by the Zimm-Rouse relationship:

$$\tau = \frac{M\eta_0[\eta]}{RT}\frac{1}{\Lambda} \qquad (1)$$

M: Molar mass of the molecule
Λ:. Form factor.
T: Temperature.
R: Constant of perfect gases.
η_0: Viscosity of the pure solvent.
η:Viscosity of the polymer in solution.
$[\eta]$: Intrinsic viscosity of the solution of the polymer given by the formula of Staudinger:

$$[\eta] = \frac{\eta}{\eta_0} = 1 + K.CM^{\alpha} \qquad (2)$$

Where K and α are constants and C is the concentration of the solution.

For de macromolecules on the long chain, we have the semi empirical relation:

$$M = 1{,}45 \,.\, 10^{8} . \tau^{3/5} \quad (3)$$

The molar mass of P3HT in solution can also be measured by SEC molecular exclusion chromatography using the following formula:

$$\ln \frac{1}{KM^{\alpha}} = a \,.\, \frac{V_e - V_0}{V_t - V_0} + b \quad (4)$$

Or a and b are constants, K and α depend on the geometry of the studied polymer

V_e: Volume of the elapsed buffer of the column before the exit of the polymer studied.

V_t:Volume of the elapsed buffer of the column before the exit of the small molecules.

V_0 : Volume of the elapsed buffer of the column before the release of very large molecules.

It is even possible to use static light scattering (SLS), gel electrophoresis, osmometry, translational diffusion, ultracentrifugation (sedimentation mass M_z), etc., to measure the molar masses on the number and on the weight of the polymer studied P3HT, which have the value:

$M_n = 22620 \ g/mol$(by SEC and osmometry)
$M_w = 33910 \ g/mol$(by SLS and SEC)

And an apparent molar mass of the macromolecule dependent on the molecular anisotropy δ by equation:

$$\delta = \sqrt{\frac{5}{4}\left(\frac{M_{app}}{M_w} - 1\right)} \quad (5)$$

The parameter $\delta$is obtained by used of flow birefringence

Table 1: Molecular masses and polydispersity index obtained by SEC in solution in polystyrene equivalent THF for the batch of P3HT from Aldrich and Rieke.

	M_n [g/mol Eq PS]	M_w [g/mol Eq PS]	I_p
P3HT lot aldrich	22 620	33 910	1.50
P3HT lot Rieke	24 180	37 590	1.50

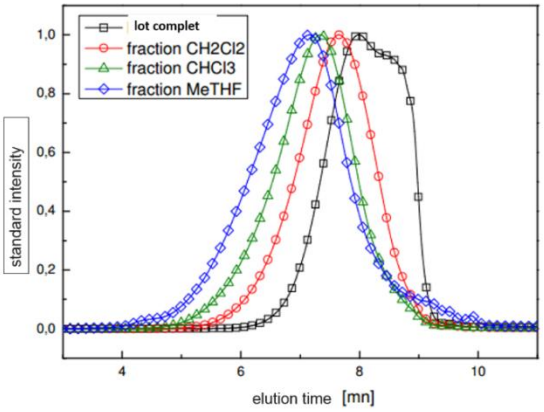

Figure 3: Chromatogram obtained for the different fractions of P3.

This chromatogram thus reveals the presence of three fractions obtained from the polymer P3 in addition to the complete p3 as a function of their elution time different can be distinguished and separated and by an optical method (spectrophotometry, differential refractometry, ...) can determine their abundance and also one can have information on the distributions of their molar masses.

2.2 Acceptor Material PCBM

Methyl [6,6] -phenyl-C61-butanoate PCBM is an electron-accepting organic semiconductor consisting of a C_{61} fullerene unit (a conventional C_{60} bearing a methylene -CH_2- laterally) substituted with a phenyl group. C_6H_5 on one side as well as with a butyric acid ester - $(CH_2)_3$-COOH and methanol CH_3OH, forming, on the other side, a methyl butyrate group - $(CH_2)_3$-COO-CH_3.

It is extensively studied in the context of polymer 2,3 photovoltaic cells to form p-n junctions with polythiophenes such as P3HT. As regards its molecular weight, it is determined either by osmometry, viscosimetry, quantitative and qualitative chemical analyzes or by mass spectrometry M(PCBM) = 910.8804 ± 0.0592 g/mol.

The PCBM is solubilized in chlorobenzene, which results in its crystallization into nanocrystals grouped together with different crystalline orientations. This crystallization depends on the nature of the solvent, in orthodichlorobenzene the polymer crystallizes in the monoclinic system, in contrast in chlorobenzene, it crystallizes in the triclinic system that promotes optimal electron transport. The covalent grafting of C_{60} fullerene with PCBM (necessary for more delocalization of electrons) is carried out by, immersing it in a

solution of C_{60} dissolved in benzene or toluene with a concentration of 1 to 4 mmol /l. Then heating the mixture under reflux under a nitrogen atmosphere for 2 to 3 days. Then rinsing the samples obtained with the pure solvent in order to remove the physiosorbed C_{60} molecules. The deposition of the PCBM is carried out on the surface of a silica substrate in order to measure the thickness by ellipsometry, formed layers that can be calculated from the following formula:

$$d = \frac{M\lambda_1\lambda_2}{2[n_1(\lambda_1)\lambda_2 - n_2(\lambda_2)\lambda_1]} \quad (6)$$

M: Number of oscillations.

λ_1 andλ_2: Wavelengths of the light passing through the solution and the substrate.

$n_1(\lambda_1)$and$n_2(\lambda_2)$ indices of refractions of the two mediums as a function of $\lambda_1 and \lambda_2$.

The experimental measurement of the thickness results in the value$d = 44\ A^{\circ}$. This shows that the growth is carried out by 4 layers from bilayers.

Also the thickness can be measured by visible UV absorption spectrophotometry by applying the Beer-Lambert law:

$$A = \alpha . d . \rho \quad (7)$$

Where A is the absorbance, α coefficient of absorption of the layer vis-a-vis the radiation, ρ the density of the layer, d the thickness of the studied layer.

The covalent grafting between PCBM and C60 fullerene leads to changes in the absorption and luminescence spectra of PCBMs that can be characterized by Fourier Transform Infrared Spectroscopy (FTIRS), so the evolution of the substrate layer can be followed by surface-excited Raman spectroscopy (SERS), this grafting is manifested by the appearance of the characteristic absorption bands in the infrared. For the visible UV spectrum, we observe the appearance of a single absorption band and this reveals a small amount of C60 presented on the layers of PCBM. The quantity of molecules on the surface remains constant as shown by ESCA (electron spectroscopy for chemical analysis) studies.

The stereochemistry of PCBMs is studied in 2D ((1H) and (13) C) NMR solutions in Deuterated solvents (CDCl3, CD2Cl2) and the morphology of the layer is characterized by Atomic Force microscopy.

The mass percentages of C60 in the PCBM are determined by thermogravimetric analysis from the mass-temperature diagrams from which the different degradation temperatures of the compound can be derived. Concerning the P3HT crystallization exotherms, the fusion endotherms are obtained by the differential scanning calorimetry as well as the melting and crystallization temperatures of the P3HT:$T_{fus} = 232.4\ °C$ and $T_{cr} = 201.5°C$

The thermal effects of crystallization and melting, the heating curves and those of the two materials were studied by microcalorimetry($\Delta H_{fus} = 20\ J/g$ and $\Delta H_{cr} = 20\ J/g$) and the differential thermal analysis, as well as the crystallinity index of P3HT expressed by:

$$\chi_c = 100.\frac{\Delta H_{fus}}{\Delta H_0} \quad (8)$$

Or

ΔH_{fus}: The enthalpy of fusion.

ΔH_0: The reference enthalpy.

3 CHARACTERIZATION AND ORGANIZATION OF THE ACTIVE LAYER P3HT-PCBM

3.1 Organization of Polymer Chains P3HT

The solubilization of P3HT in chlorobenzene is dependent on the purity of the polymer, its high molecular weight which can reach 50000 g / mol, the stoichiometry, the chemical coupling conditions (catalyst type, quantity and concentration) the reaction conditions (1). absence of oxygen, good magnetic or mechanical stirring) and finally the solubility of the monomer and the polymers in the reaction solvent. And in order to lead to a strong fibrillar organization of the P3HT chains in the form of a network leading to a high value of current density, it is necessary that the interaction between the polymer chains is more intense than their interaction with the solvent. This aggregation of chains in fibrillar structure is governed by (π_stacking) and conditioned by the structure and the chemical nature of the polymer, the interchain interactions (hydrogen bonds, π interactions, dipolar interactions...), solute solvent interactions and finally the interactions of the substrate surface with the polymer chains. The solvent of choice used for structuring chains on fibrils is p-xylene.

($T_{ebu} = 138°C;\ \mu = 0\ D\ ;\ \varepsilon = 2.3\ ;\ n_D^{(20°C)} = 1.458$)

which completely dissolves P3HT. At a temperature of 80°C. For a concentration ranging from 0.5% (wt) to 3% (wt) for one hour, which leads to an organization of the chains or fibrils under low temperature $v_{cooling} = 20°C/h$ for 4 hours in the dark, the detection of these fibrils is carried out by

visible UV spectroscopy, we observe 3 absorption bands 525 nm; 555nm; 610 nm at a concentration of 1% (wt) in p-xylene at a temperature of 80 ° C., identical to those of a P3HT film deposited by spin caoting on a glass substrate for 2 h to 48 h with v = 20 ° C./h.

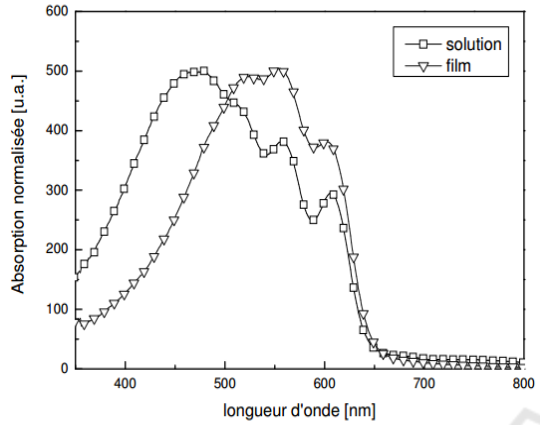

Figure 4: Normalized absorption spectra of a native solution of P3HT fibrils in p-xylene and in film form.

This makes it possible to observe a good stack of chains, thus a structure identical to that obtained in the solid phase. An increase in the absorbance with the fibril structuring explained by induced dipole-induced dipole interactions, such as, for example, London dispersion between the two chains of interaction energy:

$$U_L = -\frac{\bar{\alpha}_1 \bar{\alpha}_2 \, neE_{ox}^D}{12\pi\varepsilon r^6} \qquad (9)$$

E_{ox}^D: Donor oxidation potential (0.21V) measured electrochemically (cyclic voltammetry) or by UV and XPS spectroscopy (X-RAY PHOTO ELECTRON SPECTOSCOPY)

$\bar{\alpha}_1 \, and \bar{\alpha}_2$: Anisotropic Polarisabilities of the two chains.

ε: Dielectric constant of the solvent

r: The sum of the two Van-der-Waals radii of the two chains

e: Eelementary charge

n: Number of transferred electrons

Interactions between fibrils can occur and result in agglomeration of these which can be dispersed by agitation of the solution.

Studies of the shape of these fibrils show their lamellar organization in rod structure (measurement of diffusion constant, flow birefringence, sedimentation coefficient, electron microscopy, coefficient of friction, radius of gyration, ...) On the other hand, the transition from the disordered form to the ordered form induces a bathochromic effect which manifests a sol-gel transformation with an isobestic point of 450 nm, thus an increase in the regioregularity of the polymer, an optimization of structuration chains requires the control of the percentage of the fibrils in solution by means of centrifugation followed by filtration and deposition on the substrate by the dipping method or by the spin-coating method and according to the concentration used it is possible to obtain isolated fibrils, fibrillar networks or complete layers of morphology characterized by SEM (Scanning Electron Microscopy) and AFM (Atomic Force Microscopy): for the isolated fibrils found as dimensions: $0.5\mu m\langle L\langle 5\mu m$; $5nm\langle\varepsilon\langle 15nm$ $30nm\langle l\langle 50nm$

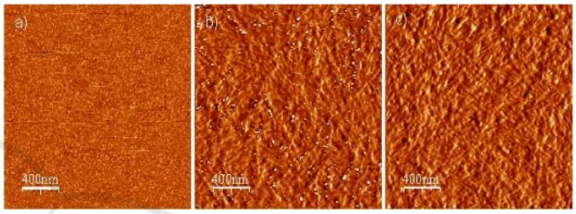

Figure 5: AFM images (non-contact tapping mode, phase contrast image, 10x10 µm) obtained on P3HT films obtained with (a) 0 wt%, (b) 75 wt% and (c) 97 wt% of P3HT fibril in solution.

Thus, the presence of the non-regioregular poly-3-alkylthiophene is observed, which leads to the conclusion that the texture of the spin-on film on the glass substrate coated with ITO (indium tin oxide) which represents the anode, is determined by the percentage of fibrils which is demonstrated by the AFM, the higher this percentage is, the higher the fibril surface concentration is important, this leads to a controlled structuring which improves further by heat treatment of P3HT (at 150 ° C. for 5 min) which doubles crystalline domains and halves the disorder, as shown by XRD(X-ray diffraction) studies on films deposited on silicon substrates, lamellar organization of fibrils with inter-lamellar distance of 16.2 A ° and a coherence length l_c of 173 A ° are observed and this is due to the small thickness of the lamellae, also the stacking fluctuations are lower than those of the unannealed P3HT, so the heat treatment results in the increase of the regular order in the fibrils.

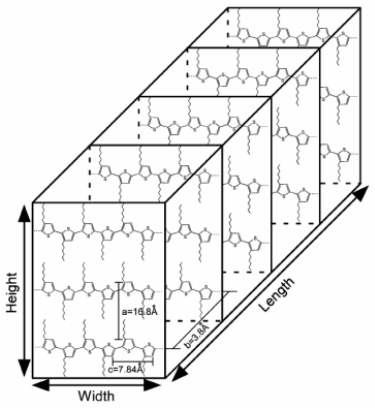

Figure 6: Simplified diagram of a regio regular P3HT fibril.

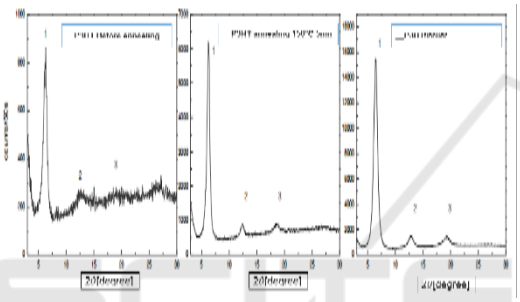

Figure 7: Wide-angle X-ray diffraction spectra on films spin coated on silicon substrates from non-fibrillar P3HT before and after annealing and from fibrillar P3HT (native solution).

Table 2: Position of diffraction peaks and associated lattice spacings for a non-annealed P3HT film, the same annealed film at 150 °C for 5 minutes and a fibrillar P3HT film, obtained on spin-on silicon substrate.

Sample	Peak number	Position [°]	Reticular distance [A°]	Disorder (%)	width at half height [rad]	Cohérence length [A°]
P3HT not annealed	001 002 003	6.22 12.78 18.96	16.48 8.04 5.43	9.5 6.7 5.5	0.013 0.047 0.091	96
P3HT anneals 150 ° C - 5 mn	001 002 003	6.22 12.39 18.55	16.49 8.30 5.55	4.5 3.2 2.6	0.0001 0.0002 0.0005	173
P3HT fibril	001 002 003	6.44 12.82 19.23	15.93 8.01 5.36	4.7 3.3 2.7	0.0141 0.0200 0.0267	115

Finally, and to close with P3HT electrochemical studies by cyclic voltammetry and electrochemical impedance spectroscopy have shown that this fibrillar organization modifies the potential for oxidation-reduction of fibrilated P3HT as well as the HOMO and LUMO energy. By cyclic voltammetry at a scanning rate of 20 mV / s, two oxidation waves are observed for the unstructured P3HT, which means the presence of two forms: one structured with low oxidation potential and the other amorphous with high potential. oxidation. As regards the fibrillated P3HT a single wave of oxidation observed therefore the presence of a single form.

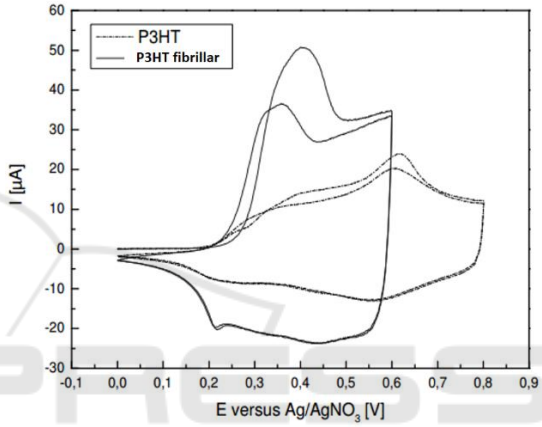

Figure 8: Voltammograms on a gold electrode of a film of P3HT and fibrillar P3HT (native fibril solution) obtained by evaporation of gold electrode drop in 0.1M [Et 4NBF4] / PC, against electrode of platinum and reference Ag / AgNO3 0.01 M in CH3CN at 20 mV.s-1.

There is a relationship between the energies of the HOMO and LUMO orbitals and the threshold redox potentials

$$E_{LUMO} = -(4.8 + E^{red}_{threshold}) \quad (10)$$

$$E^{red}_{threshold} = -2.55V$$

$$E_{HOMO} = -(4.8 + E^{ox}_{threshold}) \quad (11)$$

$E^{ox}_{threshold} = 0.22V$ these measures its calibrated compared to the ferrocene

$$\Delta E_{gap} = e\left[E^{red}_{threshold} - E^{ox}_{threshold}\right] \quad (12)$$

$$\Delta E_{gap} = -2.76 \text{ ev}$$

This three equations is very important because is represent relations between quantum chemical parameters E_{LUMO}, E_{HOMO} and electrochemical parameters $E^{ox}_{threshold}$ and $E^{red}_{threshold}$.

Table 3: Electrochemical characteristics obtained on a gold electrode of a film of P3HT and of fibrillar P3HT (native solution of fibrils) in 0.1M [Et4NBF4] / PC, against platinum electrode and reference Ag / AgNO3 0, 01M in CH3CN. E (Fc/ Fc+ = 0.062 V) in PC.

Films	$E_{ox}^{threshold}$	$E_{red}^{threshold}$	HOMO [eV]	LUMO [eV]	$\Delta E^{electrochemical}$ [eV]
P3HT	0.206	-2.552	-4.94	-2.19	2.75
fibrillar P3HT	0.239	-2.460	-5.00	-2.28	2.72

3.2 Organization of the Acceptor Donor Active Layer (P3HT-PCBM)

Donor and acceptor were mixed together after thermal annealing at 150 ° C for 5 min with the use of the wrong solvent (chlorobenzene C= 10:10 mg / ml) resulting in self-assembly of P3HT and PCBM therefore the formation of a network of one dimensional objects by induced dipole interactions of the two polymers superior to the solvent-polymer polarization interactions, thus an active layer with donor-acceptor interfaces. The presence of PCBM does not disturb the structured P3HT organization but leads to the appearance of vibronic bands (515 nm, 551 nm, 603 nm) characterizing the formation of the active layer that modify the absorption spectrum of P3HT (hyperchromic effect).

The deposition of the layer on the ITO (Indium tin oxide) anode which covers the glass substrate is done by spin-coating at 2000 rpm for 2 min, the cleaning of the substrate of the impurities is carried out by ethanol under ultrasound. The aluminum cathode is deposited by evaporation in vacuo and results in a thickness ranging from 50 nm to 110 nm, which improves the optical and electrical properties of the cathode. Thermal or microwave treatment allows segregation between polymers in the active layer. The orientation of the grating effected by an electric field perpendicular to the electrodes is due to the anisotropy of the polarizability of the molecules. The morphology of the active layer of P3HT_PCBM after heat treatment is characterized by TEM transmission electron microscopy.

Finally, the controlled morphology of the active layer leads to the increase of the potential of the open circuit V_{OC}:

$$\boldsymbol{V_{oc} = \frac{1}{e}\left(E^{d}_{HOMO} -\right)}\text{-0.3} \quad \text{V} \quad (11)$$

or $\boldsymbol{E^{a}_{LUMO} = -4.3eV}$ for the PCBM and $\boldsymbol{V_{oc} = 0.6V}$

4 CONCLUSIONS

The use of different physicochemical techniques and nanotechnology processes to characterize the electron donor and acceptor polymers allows the control at the nanometer scale of the morphology and the texture of the active layer. Optimal organization of the two materials P3HT and PC61BM, in the acceptor donor heterojunction, thus obtaining a privileged orientation of the molecular fibrils of P3HT and nano-crystals of PC60BM with respect to the electrodes, it is furthermore advantageous to macroscopically transfer the This is due to the stacking of the polymer chains and the weak coupling between them, which further optimizes inter-charge transfer at the expense of intrachain transfer, which can hardly lead to a macroscopic transfer of charge and thus to usable electric currents.

And this is of course considered as a step in advance of the molecular nanoelectronics that eclipses day by day and that relegates in the shadows conventional microelectronics derived from silicon and inorganic semiconductors.

REFERENCES

Alet, P.-J. *et al.* (2006) 'Hybrid solar cells based on thin-film silicon and P3HT: A first step towards nano-structured devices*', *The European Physical Journal Applied Physics*, 36(3), pp. 231–234. doi: 10.1051/epjap:2006145.

Baran, D. *et al.* (2017) 'Reducing the efficiency–stability–cost gap of organic photovoltaics with highly efficient and stable small molecule acceptor ternary solar cells', *Nature Materials*, 16(3), pp. 363–369. doi: 10.1038/nmat4797.

Berson, S. *et al.* (2007) 'Elaboration of P3HT/CNT/PCBM Composites for Organic Photovoltaic Cells', *Advanced Functional Materials*, 17(16), pp. 3363–3370. doi: 10.1002/adfm.200700438.

Björström, C. M. *et al.* (2005) 'Multilayer formation in spin-coated thin films of low-bandgap polyfluorene:PCBM blends', *Journal of Physics: Condensed Matter*, 17(50), pp. L529–L534. doi: 10.1088/0953-8984/17/50/L01.

Brabec, C. J. *et al.* (2010) 'Polymer-Fullerene Bulk-Heterojunction Solar Cells', *Advanced Materials*, 22(34), pp. 3839–3856. doi: 10.1002/adma.200903697.

Chen, D. *et al.* (2011) 'P3HT/PCBM Bulk Heterojunction Organic Photovoltaics: Correlating Efficiency and Morphology', *Nano Letters*, 11(2), pp. 561–567. doi: 10.1021/nl103482n.

Dang, M. T., Hirsch, L. and Wantz, G. (2011) 'P3HT:PCBM, Best Seller in Polymer Photovoltaic Research', *Advanced Materials*, 23(31), pp. 3597–3602. doi: 10.1002/adma.201100792.

Destruel, P. and Seguy, I. (2007) 'Les cellules photovoltaïques organiques', *Reflets de la physique*, (6), pp. 16–18. doi: 10.1051/refdp/2007064.

Peumans, P., Yakimov, A. and Forrest, S. R. (2003) 'Small molecular weight organic thin-film photodetectors and solar cells', *Journal of Applied Physics*, 93(7), pp. 3693–3723. doi: 10.1063/1.1534621.

Rispens, M. T. *et al.* (2003) 'Influence of the solvent on the crystal structure of PCBM and the efficiency of MDMO-PPV:PCBM "plastic" solar cells', *Chem. Commun.*, (17), pp. 2116–2118. doi: 10.1039/B305988J.

Vanlaeke, P. *et al.* (2006) 'P3HT/PCBM bulk heterojunction solar cells: Relation between morphology and electro-optical characteristics', *Solar Energy Materials and Solar Cells*, 90(14), pp. 2150–2158. doi: 10.1016/j.solmat.2006.02.010.